

Retrieving Profile Temperatures in a Frozen Topsoil Near the TFS, Alaska, Based on SMOS Brightness Temperatures at the 1.4-GHz Frequency

Valery L. Mironov, *Member, IEEE*, Konstantin V. Muzalevskiy, *Member, IEEE*, and Zdenek Ruzicka

Abstract—In this paper, the method previously proposed in earlier work for measuring the temperature profile in a frozen topsoil using multiangular brightness temperature observations in the L-band has been experimentally tested. At a frequency of 1.4 GHz, full-polarization multiangular brightness temperature data were obtained from the Soil Moisture and Ocean Salinity (SMOS) satellite land product of Level 1C, with the SMOS footprint being centered at the Toolik Field Station (TFS), Alaska. The SMOS data covered the period from January 1, 2010 to December 31, 2011. Retrieval of the temperature profiles in a frozen topsoil was based on the semiempirical emission model L-MEB and the temperature-dependent dielectric model for an organic-rich tundra soil. The soil samples measured to develop the dielectric model were collected at the TFS site. For winter seasons, the retrieved temperature profiles in the 16.0-cm topsoil were validated relative to the temperature profiles measured *in situ*. As a result, the values of root-mean-square error and determination coefficient of the temperatures retrieved at the depths of 0.6, 8.7, and 16.0 cm, relative to the respective temperatures measured *in situ*, were found to be 2.8 °C, 4.9 °C, and 6.4 °C and 0.62, 0.42, and 0.26, respectively. The sources of error and possible improvements of the proposed retrieving algorithm were discussed. The major result of this study is the demonstration of the potential possibility for remote sensing of the temperature profile in a frozen arctic topsoil using the SMOS multiangular brightness data.

Index Terms—Microwave radiometry, remote sensing, soil measurements, temperature measurement.

I. INTRODUCTION

THE temperature profiles in the active layers of the permafrost zone play a crucial role in governing energy fluxes between the soil and the atmosphere and, thus, determine the processes of permafrost degradation accompanied by carbon dioxide and methane release. At the same time, the weather station networks in the northern latitudes are too sparse to provide sufficient data of the active-layer temperature profiles. Therefore, satellite remote sensing is a highly demanded information technology for monitoring the temperature of the

active permafrost layer. Previously published results on this topic [1], [2] reveal the remarkable results of employing remote sensing to measure the soil temperature at tundra and forested test sites located in the northern territories of the United States and Canada. In [1], the values of land surface temperature (LST) were obtained with the use of the Moderate Resolution Imaging Spectroradiometer (MODIS) and compared with the values of the ground surface temperature (GST) measured *in situ* by meteorological stations at a depth of 3–5 cm. The observations were conducted at 12 test sites during the period from 2000 to 2008. Thus, obtained values of the LST deviated from the *in situ* measured values of the GST by 4.4 °C–14.7 °C in terms of root-mean-square error (rmse), and the determination coefficient (R^2) varied in the range from 0.49 to 0.92. It is worth noting that these estimates correspond to clear weather conditions of observation, as any cloud coverage completely impedes LST observations with the infrared sensor MODIS.

In [2], the values of the effective ground surface temperature (EGST) were obtained with the use of the Advanced Microwave Scanning Radiometer—Earth Observing System (AMSR-E), working in the frequency range from 6.9 to 89 GHz and compared with the values of GST measured *in situ* by meteorological stations in the topsoil layer at a depth range of 0–8 cm. The observations were conducted at seven test sites located in the northern territories of the United States and Canada during the period from 2002 to 2004. For nonforested sites, the obtained values of the EGST deviated from the values of *in situ* measured GST by 2.2 °C–10.5 °C in terms of rmse, and R^2 varied in the range from 0.24 to 0.77. The major result of the research conducted in [1] and [2] is the demonstration of the potential possibility for remote sensing of the topsoil temperature using the data of the brightness of the earth surface taken using the MODIS and AMSR-E missions. Meanwhile, when using the AMSR-E observations, the depth of sensing, which is on the order of thermal emission layer depth, is limited by 0.5–2.8 cm in the case of thawed soil, as was noted in [2], and, most probably, may not exceed 6 cm in the case of frozen soil, according to [3]. In the case of MODIS observations, emission depth is limited by the skin of the ground surface.

Therefore, the objectives of increasing the sensing depth and retrieving a temperature profile in the arctic topsoil, at least in the case of frozen soil, are actualized. In this respect, the data provided by the Soil Moisture and Ocean Salinity (SMOS) mission may pave the way for reaching this goal. As was shown in [4], the brightness temperatures measured *in situ* by the radiometer ELBARA, at a frequency of 1.4 GHz,

Manuscript received March 27, 2014; revised September 8, 2014, March 4, 2015, November 23, 2015, and June 21, 2016; accepted August 2, 2016. Date of publication August 31, 2016; date of current version September 30, 2016. This work was supported by the Russian Science Foundation through Project 4-17-00656.

The authors are with Kirensky Institute of Physics, 660036 Krasnoyarsk, Russia, and also with Siberian State Aerospace University, 660037 Krasnoyarsk, Russia (e-mail: rsdvm@ksc.krasn.ru; rsdkm@ksc.krasn.ru; tramtara@seznam.cz).

Digital Object Identifier 10.1109/TGRS.2016.2599272

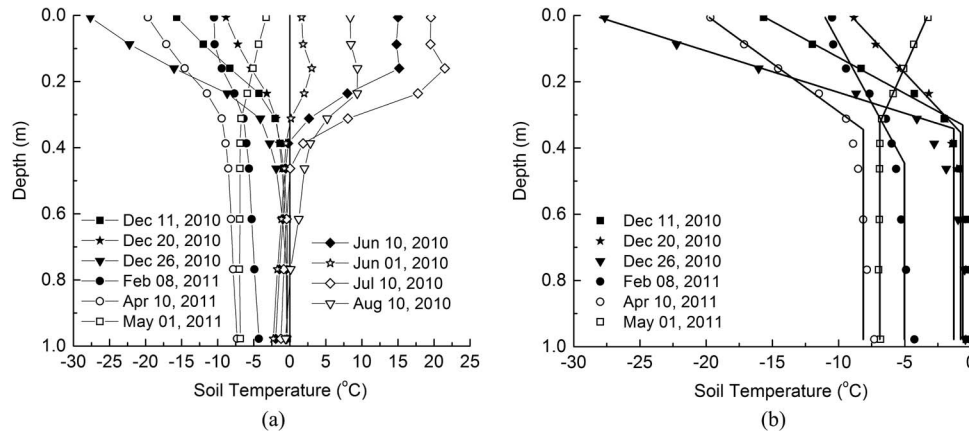


Fig. 1. (a) Typical temperature profiles in the topsoil measured at the TFS during 2010–2011. (b) Approximation of the typical temperature profiles in wintertime, with using piecewise linear function (4).

used in the SMOS mission revealed noticeable variations in the course of freezing of the topsoil layer down to 30 cm. These observations conducted in a forested area located in Northern Finland indirectly confirm that the brightness temperature taken from the SMOS radiometer in the winter season is formed due to emission from the topsoil frozen layer of approximately 30 cm in depth. In principle, the possibility of estimating a temperature profile within this layer in the winter season is based on the fact that the emission from the topsoil decreases as the thickness of the emitting layer (depth of sensing) decreases with the increase in the observation angle. Indeed, with the positive temperature gradient in the topsoil in the winter season, a thinner emitting layer (corresponding to a larger observation angle) has a lower average physical temperature, relative to a thicker emitting layer (corresponding to the nadir observation angle), which contains lower and, therefore, warmer soil layers.

A theoretical feasibility study of such a remote sensing technique was conducted in [5]. For this purpose, an extremely simplified model was selected. First, a type of topsoil was assumed to be homogeneous both in depth and over the area occupied by the SMOS footprint. Second, the relief was assumed to be flat, and as in an idealized case, no water objects were suggested to be present within a footprint. Moreover, there were no snow and vegetation covers above the topsoil. In the course of studies in [5], the brightness temperatures were simulated, as if they were measured by the SMOS radiometer. For this purpose, the bare soil emissivity model suggested in [6] and the temperature-dependent dielectric model of organic-rich arctic soil [7] were used. Moreover, the data on soil moisture, dry soil density, and temperature profiles measured by the Biosphere Station Franklin Bluffs (69°39' N, 148°43' W) from 1999 to 2001 were employed. Based on the simulated angular patterns of brightness temperatures, as if taken by the SMOS radiometer, the surface soil temperature and the temperature gradient were retrieved by minimizing the residual norm between the simulated brightness temperatures and those calculated with the simplified thermal radiation model, as outlined above. Moreover, a linear temperature profile was used in the brightness temperature model. In [5], the temperature profiles in the topsoil, i.e., the 15-cm layer, were retrieved with the rmse at 0.9 °C. Keeping in mind the extreme simplifications

in [5], this approach needs to be tested in real conditions, at least to clarify its principal applicability to deriving the temperature profile in the arctic topsoil.

In this paper, the methodology developed in [5] was applied to retrieve temperature profiles in the arctic topsoil based on the SMOS multiangular brightness temperature patterns. For a test site, the area centered at the Toolik Field Station (TFS) in North Slope, Alaska (68.6275 N, 149.5950 W) was employed. The temperatures at depths of 0.6, 8.7, and 16 cm were derived using the SMOS data spanning from January 1, 2010 to December 31, 2011, and the deviations in terms of rmse of the derived temperatures from those measured *in situ* were estimated. The emission depth dramatically dropped in the case of thawed soil, and we mainly focused on testing the methodology proposed in [5] in the case of frozen soil, with the depth of freezing more than thickness of the skin layer.

II. TEST SITE AND DATA

A. Test Site and In Situ Data Measurements

The area of the TFS was chosen as a test site. This choice is due to the following two factors. First, the temperature-dependent dielectric model developed in [7] is based on the soil samples collected at this site. Second, the *in situ* measured data of the temperature and moisture profiles appeared to be easily available in [8], as well as the SMOS radiometric data.

The weather station at the TFS monitors daily-average air temperature; precipitation; soil temperature at the depths of 0.6, 8.7, 16.0, 23.6, 31.2, 38.7, 46.3, 61.6, 76.8, and 97.8 cm; and soil water content at the depths of 9, 12, 38, 39, and 68 cm [8]. As an example, in Fig. 1, some temperature profiles relevant to the winter and summer seasons are shown, demonstrating that the temperature dependence relations in the layer at a depth of 23.6 cm are close to linear ones in wintertime, whereas the temperature is nearly constant in this layer in the summer time. The landscape in the TFS area is classified as a dry heath and moist tussock tundra covered with sedges, mosses, deciduous, and evergreen shrubs [9]. The soil is typical Aquiturbel, with the thickness of the organic layer varying from 4 to 20 cm and with the average bulk density of dry organic soil varying from

0.08 to 0.36 g/cm³ [10]. The average bulk dry density of the subjacent mineral horizon varies from 0.44 to 1.28 g/cm³ [10]. Furthermore, at modeling, we will assume that the active layer of the soil is composed of only organic matter. The thickness of the active layer is approximately 50 cm, and the maximal thickness of the snow layer varies from 20 to 40 cm [9].

B. SMOS Remote Sensing Data

The 2-D interferometric radiometer on board the SMOS measures the brightness temperature of the earth surface at vertical and horizontal polarizations in the range of viewing angles from 0° to 65°, with a spatial resolution of 43 km × 43 km [11]. The multiangular brightness temperature observations of the SMOS Discrete Global Grid (DGG) node closest to the TFS test site were used. The SMOS Level-1C land full-polarization product (MIR_SCLF1C) was used for the descending overpasses at 4 A.M. to 6 A.M. (UTC), for winter seasons only, from January 1, 2010 to December 31, 2011, and included daily records. In the period of observations, the radiometric accuracy of the SMOS brightness temperatures varied from 2.0 K to 9.1 K in the entire range of viewing angles and for both the *H*- and *V*-polarizations. These estimates are based on the data block «Pixel_Radiometric_Accuracy» of the SMOS Level-1C product. The fully polarimetric SMOS data were converted from the antenna reference frame [XY] into the surface level frame [HV]. For this purpose, the transformation matrix was used [12] together with the Faraday and geometric rotation angles, which were taken from the SMOS Level-1C product. The radio frequency interference filtering procedure for the SMOS data was not used.

The dependence relations of the brightness temperature on the viewing angle, measured by using SMOS in the range from 25° to the maximum available values (approximately 60°), were chosen for the retrieving algorithm. Values of the brightness temperature at angles less than 25° were discarded because the brightness temperatures on the vertical and horizontal polarizations coincided with each other within the range of radiometric error, and they did not give any dependence relations from viewing angles. Approximately 70 viewing angles were available in the range from 25° to 60°. The initial values of the brightness temperature were smoothed using the adjacent-averaging method over a sliding window containing 5–10 initially measured values. The initial and smoothed values of the brightness temperature are depicted in Fig. 2. The smoothed values of the brightness temperatures as a function of time for the *V*- and *H*-polarizations, which were measured at a viewing angle of approximately 40°, are shown in Fig. 3. This value of the viewing angle was chosen as some angle that is practically used for spaceborne instruments, for example, on the Soil Moisture Active Passive satellite. As an example, only one calendar year period of time is shown just to demonstrate the variations in brightness temperature observed during all seasons of the year. According to the TFS data, the soil was in the process of freezing and thawing in the periods of September 19–21, 2010 and May 13–17, 2011, respectively. In Fig. 3, these periods are marked with vertical dashed lines around which a sharp increase and decrease in brightness

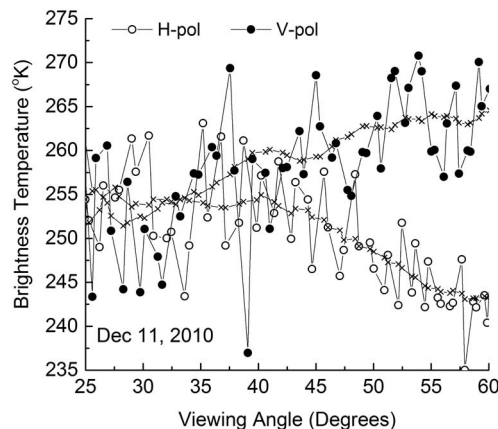


Fig. 2. Dependence relations of the viewing angle of the SMOS brightness temperature. Open and filled circles correspond to the initially measured values. The crosses represent the averaged values.

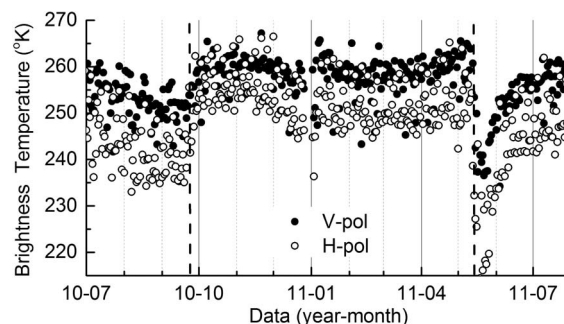


Fig. 3. Time series of the brightness temperature at a viewing angle of 40°. The periods of soil freezing (September 19–21) and thawing (May 13–17) are marked with vertical dashed lines (compare with the *in situ* measured temperature data shown in Fig. 5).

temperature are observed, respectively, indicating the processes of soil freezing and thawing. According to the work in [5], to derive the temperature profiles with the use of the brightness temperature data, we will use the microwave emission model outlined in the following section.

III. MICROWAVE EMISSION MODEL OF ARCTIC SOILS

To model the brightness temperature $T_{B,p}^{th}(\theta)$ as a function of viewing angle θ for the horizontal, i.e., $p = H$, and vertical, i.e., $p = V$, polarizations, we used the semiempirical model for microwave emission in the case of bare soil introduced in [13] and further developed in [14], i.e.,

$$T_{B,p}^{th}(\theta) = \eta_p(\theta) \cdot T_{\text{eff}}(\theta). \quad (1)$$

Here, $\eta_p(\theta)$ and $T_{\text{eff}}(\theta)$ are the emissivity and effective temperature, respectively. In its turn, according to the work in [14], the emissivity $\eta_p(\theta)$ is a function of the Fresnel reflection coefficient $R_p(\theta)$ and the soil surface roughness parameter $Z_s = \sigma^2/L_c$, with σ and L_c being the height of roughness, in terms of standard deviation, and the autocorrelation length of roughness, respectively. The formula for emissivity as a

function of $R_p(\theta)$ and Z_s can be presented in the following form:

$$\begin{aligned} n_p(\theta) &= 1 - [(1 - Q)|R_p(\theta)|^2 + Q|R_q(\theta)|^2] e^{-H_r \cos^{N_p} \theta} \\ Q &= 0.1771H_r \\ N_H &= 1.615(1 - e^{-H_r/0.359}) - 0.238 \\ N_V &= 0.767H_r - 0.099 \\ H_r &= \begin{cases} 2.615(1 - e^{-Z_s/2.473}), & Z_s \leq 1.235 \\ 1.0279, & Z_s > 1.235 \end{cases} \end{aligned} \quad (2)$$

Combinations $p = H, q = V$ and $p = V, q = H$ are possible. The Fresnel reflection coefficient in (2) suggests a smooth surface of the soil. It should be considered as a functionality of the complex relative permittivity profile $\varepsilon_s(z)$. Provided a known profile $\varepsilon_s(z)$, it can be calculated by using the iteration method [15]. Parameter Q may be interpreted as a depolarization factor, which accounts for polarization mixing effects. According to the work in [13], the effective temperature $T_{\text{eff}}(\theta)$ in (1) can be expressed as the following functionality:

$$T_{\text{eff}}(\theta) = \int_0^{\infty} T(z) \frac{k_0 \kappa_s(z)}{\cos(\theta)} \exp \left[- \int_0^z \frac{k_0 \kappa_s(z')}{\cos(\theta)} dz' \right] dz \quad (3)$$

where $T(z)$ is a temperature profile in the soil, $k_0 = 2\pi f/c$ is the free-space wavenumber, c is the light velocity, f is the wave frequency, and $\kappa_s(z) = \text{Im} \sqrt{\varepsilon_s(z)}$ is the normalized attenuation coefficient. It is evident that the profiles $T(z)$ and $\varepsilon_s(z)$ must be consistent with each other. The largest error of 6.3 K of models (1)–(3) was estimated from the experiments [14, Table 2] carried out with predominantly mineral solids in the thawed condition, with respect to only one specific location (PORTOS 1993 data set, Avignon, France). Models (1)–(3) do not take into account the effects of scattering and attenuation caused by the snow and vegetation layers. Moreover, models (1)–(3) do not take into account the relief of the test site, which is actually a moderate hilly terrain, according to the SMOS Level-2 product. As shown in [16], such simplification of the relief causes an error on the order of 0.1 K–2 K, which lies in the limits of the SMOS brightness measurement error. The retrieval error of soil temperature profiles due to the assumed approximations in the brightness temperature models (1)–(3) is a constituent of a total retrieval error. The latter will be evaluated by comparing the temperature profiles retrieved from SMOS data with the respective ground-based measurements in Section IV. The method of retrieving the soil temperature profiles with the use of the brightness temperature models (1)–(3) will be outlined in the next section.

IV. METHOD OF RETRIEVING THE TEMPERATURE PROFILE

As in [5], for developing the temperature-profile-retrieving algorithm, the temperature-dependent complex dielectric permittivity (CDP) model introduced in [7] was used. The model in [7] was developed based on the measurements conducted for the organic-rich soil samples collected at the TFS site. The soil samples contained 87% organic matter, 8% quartz, and 5% calcite. This model allows for the calculation of the CDP of soil, i.e., $\varepsilon_s(z) = \varepsilon_s(\rho_d, m_g, T(z), f)$, as a function

of dry bulk density ρ_d , gravimetric moisture m_g , temperature $T(z)$, and frequency f . The model in [7] ensures predictions of the real and imaginary parts of the relative CDP in the ranges of $0.0 \text{ g/g} < m_g < 0.98 \text{ g/g}$, $-30 \text{ }^\circ\text{C} < T < 25 \text{ }^\circ\text{C}$, and $0.5 \text{ GHz} < f < 15 \text{ GHz}$, the latter including the SMOS frequency of 1.4 GHz. At that, the standard deviation of the predictions from the measured values was shown to be 0.17. The dielectric model in [7] was derived on the basis of CDP measurements of soil samples during the freezing process. Here, the soil samples froze at $-6 \text{ }^\circ\text{C}$ in the measuring cell. When calculating the CDP with the help of the model in [7], the modified temperature scale ($T = T + 6 \text{ }^\circ\text{C}$) was used to set a temperature of freezing equal to $0 \text{ }^\circ\text{C}$.

It can be shown that, in wintertime, the measured *in situ* typical temperature profile from December 11, 2010 to May 1, 2011, as shown in Fig. 1(b), can be fitted to the piecewise linear function, i.e.,

$$T_p(z) = \begin{cases} T_s + T_g z, & z \leq z_L \\ T_s + T_g z_L, & z \geq z_L \end{cases} \quad (4)$$

Here, T_s and T_g are the surface temperature and the temperature gradient, respectively, and z_L is a salient point in which the temperature for depths below $z = z_L$ is equal to the constant value $T_s + T_g \cdot z_L$. In this case, the variations in rmse, determination coefficient, and the salient point were found to be from $0.1 \text{ }^\circ\text{C}$ to $0.9 \text{ }^\circ\text{C}$, from 0.957 to 0.998, and from 0.32 to 0.45 cm, respectively. We define the thickness of the topsoil ($0 - z_s$) in which the soil temperature variations have the most contribution into variations in brightness temperature. To this end, the difference between the values of brightness temperatures was calculated for the measured *in situ* temperature profiles $T_m(z)$, $0 < z < 97.8 \text{ cm}$ (as depicted in Fig. 1) and the temperature profiles $T(z) = T_m(z)$ if $0 < z < z_s$, $T(z) = T_m(z_s)$ if $z_s < z < 97.8 \text{ cm}$. The calculations were made for 482 soil temperature profiles, which were measured by TFS in the winter from January 1, 2010 to May 21, 2010, from September 22, 2010 to May 12, 2011, and from September 21 to December 31, 2011. It turned out that, in about 95% of cases, this difference appeared to be less than 3% when $z_s \geq 16 \text{ cm}$. Thus, following for the theoretical estimation, the salient point in (4) was chosen equal to $z_L = 16 \text{ cm}$ for calculating the brightness temperature, conducted in the process of the soil temperature retrievals. As a result, according to (1)–(4), the brightness temperature $T_{B,p}^{th}(\theta)$ in (1) can be represented as a function of the following variables:

$$T_{B,p}^{th}(\theta) = T_{B,p}^{th}(\theta, \rho_d, m_g, T_s, T_g, Z_s). \quad (5)$$

The retrieving algorithm was based on minimizing the norm of the difference between the measured $T_{B,p}^m(\theta_{p,i})$ and simulated $T_{B,p}^{th}(\theta_{p,i})$ brightness temperatures, as given by (5), i.e.,

$$F = \sum_{p=H,V} \sum_{i=1}^{N_p} \left| \frac{T_{B,p}^m(\theta_{p,i}) - T_{B,p}^{th}(\theta_{p,i})}{\sigma T_{B,p}(\theta_{p,i})} \right|^2 \quad (6)$$

where N_p is the total number of viewing angles in the range of $25^\circ \leq \theta_{p,i} \leq 60^\circ$, and $\sigma T_{B,p}(\theta_{p,i})$ is the radiometric error,

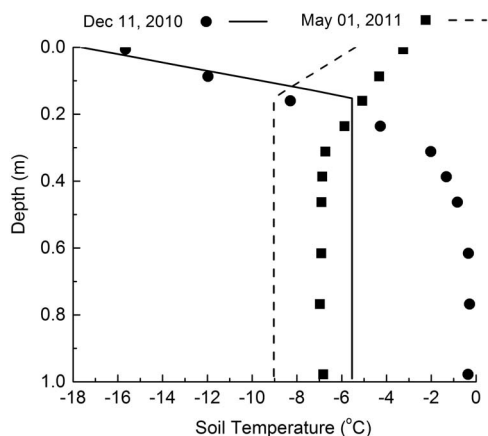


Fig. 4. Characteristic temperature profiles measured at the TFS (symbols) and retrieved from the SMOS data (solid and dashed lines), based on the proposed method.

which was taken from the Level-1C SMOS data. Both polarizations, i.e., vertical ($p = V$) and horizontal ($p = H$), are taken into account in the norm (6). The values $\theta_{V,i}$ and $\theta_{H,i}$ refer to the viewing angles' data corresponding to the vertical and horizontal polarizations, respectively. To minimize the norm, the Levenberg–Marquardt algorithm [17] was applied. In minimizing the norm of (6), a gravimetric soil moisture $m_g = m_v / \rho_d$ was calculated using the average value of volumetric soil moisture ($m_v = 0.45 \text{ cm}^3/\text{cm}^3$), which was derived from TFS data for the summer seasons of 2010 and 2011. From January 1, 2010 to December 31, 2011, in wintertime, SMOS observations for 307 days were processed from 482 available observations. The remaining data were rejected because the rmse values between the measured and modeled dependence relations of viewing angles of brightness temperatures were more than the mean radiometric accuracy of the SMOS brightness temperature observations ($\sim 5.5 \text{ K}$).

Finally, four values were derived from minimizing the residual norm (6), that is, ρ_d , Z_s , T_s , and T_g . For the parameters to be retrieved, the following initial values were set: $Z_s = 1.0 \text{ cm}$, $\rho_d = 0.4 \text{ g/cm}^3$, $T_s = -10 \text{ }^\circ\text{C}$, and $T_g = 0 \text{ }^\circ\text{C/m}$. Based on the retrieved values of T_s , T_g , and (4), the temperature in an active layer in the range of $0 \leq z \leq 16 \text{ cm}$ can be calculated at any depth. At that, the error in temperature at various depths is expected to be different and may increase with depth, as shown in Section V.

V. RESULTS AND DISCUSSION

A. Soil Temperature Retrieval

As an example, for the periods of soil surface cooling (December 11, 2010) and heating (May 1, 2011), the “retrieved temperatures” and *in situ* measured temperature profiles are shown in Fig. 4. Here and in the following, the values of soil temperature referred to as “retrieved temperatures” should be understood as those calculated at a given depth with using (4) in which parameters T_s and T_g are retrieved, as outlined in Section IV. As shown in Fig. 4, in the 16-cm-deep topsoil layer, good correspondence is observed between measured and retrieved soil temperature profiles. The soil temperatures at the

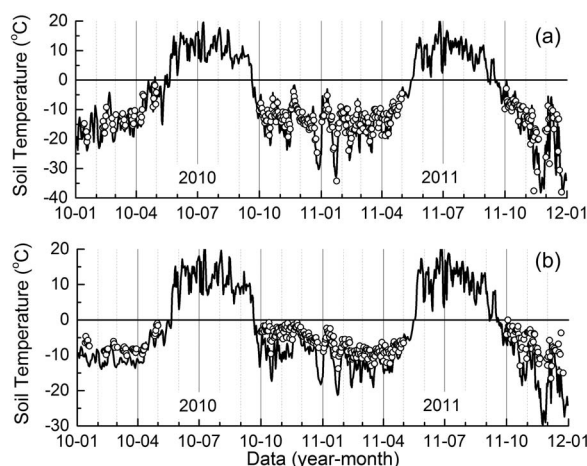


Fig. 5. Soil temperatures measured *in situ* at the TFS at the depths of (a) 0.6 cm and (b) 16.0 cm (solid lines) and the respective values retrieved from the SMOS data (open circles).

depths of 0.6 and 16.0 cm, both measured at the TFS and retrieved using SMOS brightness temperatures, are shown in Fig. 5 as a time series with respect to the whole period of observations. In Fig. 5, the retrieved temperatures at the depths of 0.6 and 16.0 cm were calculated with the use of the retrieved values of T_s , T_g , and (4). As shown in Fig. 5, at a depth of 0.6 cm, the retrieved temperatures are in good correlation with the temperatures measured *in situ*. Meanwhile, the temperatures retrieved at a depth of 16 cm are markedly shifted toward higher values relative to the temperatures measured *in situ*. The retrieved temperatures are not presented in Fig. 5 for the periods September 19–21, 2010, September 16–20, 2011, May 20–22, 2010, and May 13–17, 2011. In the course of these periods, the rmse values between the measured and modeled dependence relations of the viewing angles of brightness temperatures were more than the mean radiometric accuracy of the SMOS brightness temperature observations ($\sim 5.5 \text{ K}$), and retrieved parameters were rejected. Along with the values of topsoil temperatures, the values of soil roughness parameter Z_s and dry soil bulk density ρ_d were retrieved. Their values and standard deviations were found to be as follows: $Z_s = 0.9 \pm 0.3 \text{ cm}$ and $\rho_d = 0.18 \pm 0.09 \text{ g/cm}^3$. The retrieved value of dry soil density was found to be close to the value $\rho_d = 0.22 \text{ g/cm}^3$ measured *in situ* in a 20-cm layer [10, Table 19 b].

In Fig. 6, the retrieved temperatures, i.e., T_{SMOS} , are shown versus the *in situ* measured temperatures, i.e., T_{WS} , at depths of 0.6, 8.7, and 16.0 cm, alongside the model $T_{\text{SMOS}} = T_{\text{WS}}$. As shown in Fig. 6, the bias of the retrieved temperatures relative to the *in situ* measured ones increases with depth. To quantitatively estimate an error of the proposed retrieval method, we calculated the rmse and R^2 relative to the model $T_{\text{SMOS}} = T_{\text{WS}}$. The results of these estimations are shown in Table I, together with the respective values regarding the observations carried out with the MODIS infrared radiometer [1] (in a snow-free period) and the AMSR-E microwave radiometer [2] (in winter period) for qualitative comparison. In the case of the AMSR-E instrument, only the minimum values of rmse and R^2 are presented in Table I. In Table I, the values of rmse and R^2 relating to 1) the MODIS radiometer [1] and 2) the AMSR-E

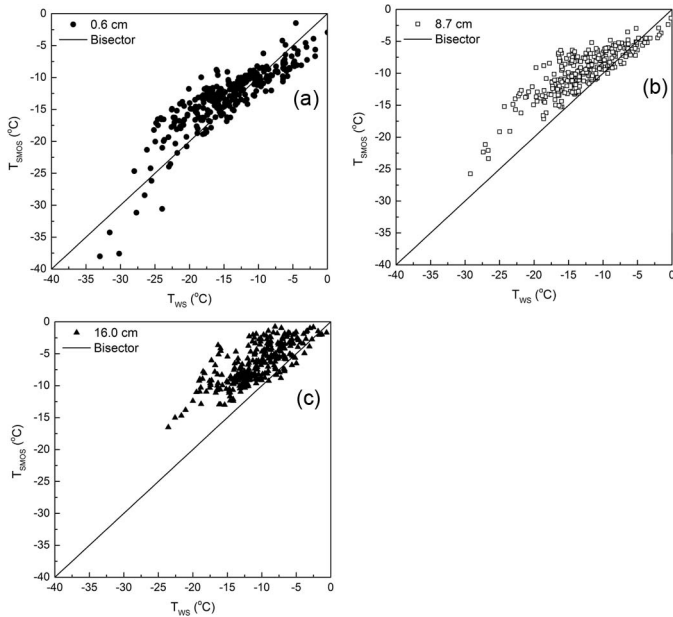


Fig. 6. Correlation of the soil temperatures retrieved at depths of 0.6, 8.7, and 16.0 cm with the SMOS data, i.e., T_{SMOS} , and with the data obtained by *in situ* measurement, i.e., T_{WS} .

TABLE I
VALIDATION STATISTICS

Depth (cm)	SMOS		MODIS		AMSR-E	
	RMSE (°C)	R ²	RMSE (°C)	R ²	RMSE (°C)	R ²
0.6	2.8	0.62				
8.7	4.9	0.42	8.5	0.61	5.5	0.5
16.0	6.4	0.26				

radiometer [2] represent the correlation characteristics between 1) the LSP values delivered by the MODIS and the *in situ* measured temperatures at a depth of 3–5 cm and 2) the effective soil temperature delivered by the AMSR-E and the *in situ* measured temperatures at a depth of 0–8 cm. The MODIS and AMSR-E data given in Table I correspond to the Imnaviat test site (68.6336 N, 149.3459 W) and the Happy Valley (69.1466 N, 148.8483 W) test site, respectively. Both of these test sites have similar physiographic factors compared with the TFS (68.6275 N, 149.5950 W), over which the soil temperatures were retrieved using the SMOS data. A direct comparison of the proposed method of soil temperature retrieval from SMOS data with the approaches used in [1] and [2] is not possible, due to the fact that the sensing of soil temperature in [1] and [2] and in this paper was carried out under different conditions. First, the validation data in [1] and [2] include a significantly longer (by a factor of 1.5–3) time span, thus covering a much wider range of the temporal variability in the environment than in the case under consideration. Second, the statistics relating to the largest retrieval errors occur during the period of freeze–thaw transitions are excluded from our analysis. Therefore, a comparison of these errors of soil temperature retrieval makes sense only on the order of magnitude. On the other hand, it is worth mentioning that, in contrast to the approaches in [1] and [2], the technique used in this study demonstrated a potential possibility to give estimates of the topsoil temperatures at different depths (0–16 cm) based on a physical model of soil thermal emission in the microwave band. For that, the thermal emission

model was used in its simplest form, with many substantial factors having been ignored, which has inevitably increased the error of temperature retrievals. In particular, in the brightness models (1)–(3), such factors as the inhomogeneity (in terms of its organic and mineral contents) of the topsoil in depth and over the area of the SMOS footprint, the impact of relief, the presence of natural water objects, and vegetation and snow covers, including the effects of dry snow and the processes of snow melting, should have been taken into consideration.

B. Possible Improvements of the Retrieval Algorithm

Let us consider in more detail some of the factors that should be taken into account in the brightness temperature models (1)–(3) to improve the accuracy of the retrieved temperature.

First, in models (1)–(3), the solid particle contents of the soil are assumed to be homogeneous with depth, whereas the actual topsoil may contain not only organic but also mineral particles, with their percentages being varied. Moreover, the vertical profile of soil moisture may also vary with depth, in contrast to the constant values of moisture assumed in models (1)–(3). Moreover, the topsoil may horizontally vary in mineral and organic contents within the limitations of pixels. Therefore, an adequate analysis in the future must be based on a set of dielectric models related to organic [18], mineral [19], and mixed soil types [20].

Second, among other factors, the error of soil temperature retrieval is caused by the influence of random variation in density, moisture, and height of the snow cover within the SMOS pixel. As shown both theoretically [21] and experimentally [22], within SMOS viewing angles, the variations in brightness temperature for horizontal polarization even in case of dry snow cover can reach about 12 K. However, as shown in Fig. 3, the total variations in brightness temperature for horizontal polarization in the winter period are about 20 K, which may include contributions of both the temperature variations of the soil and the changes in the snow cover. As can be seen from this estimate, the effect of the snow cover is essential and may reach half of the observed variations in brightness temperature in wintertime. Therefore, ignoring the snow cover factor in the brightness temperature equations (1)–(3) may result in the scatter of the retrieved values of temperature, which is observed in Fig. 6. To take into account influence of dry and wet snow cover in (1)–(3), the approaches developed in [21]–[23] could be applied.

Third, the vertical structure of freezing or thawing soil, in particular, should have been taken into consideration in the brightness modes (1)–(3) to account for most large-amplitude and fast-in-time brightness temperature variations. In [24], the path of the correct account of soil permittivity profile in the transition zone between the frozen and thawed layers is shown, but applicability of the approach [24] in the proposed method of the soil temperature retrieval requires further investigation.

Fourth, another source of error is the assumption that in wintertime, soil moisture was set equal to the mean value of soil moisture in the summer time. Nevertheless, it should be noted that the model in [7] correctly describes the complex dielectric constant and the quantitative ratio of ice and unfrozen water in

the frozen soil in the process of decreasing and increasing soil temperature for a given initial volumetric soil moisture before freezing when soil is thawed.

Fifth, natural water objects with open water or covered with ice and snow that partly occupy the SMOS footprint also modify the SMOS brightness temperature. Water accounting can be carried out in a manner similar to the method presented in [25].

Taking into account all the discussed factors in the emission, models (1)–(3) will improve the accuracy of retrievals as the model of soil thermal emission is more adequately tuned to the environmental conditions. We plan to perform this research in the future.

VI. CONCLUSION

The main objective of this paper is to conduct experimental testing of the method theoretically worked out in [3] for measuring the temperature profiles in an arctic tundra topsoil through the winter seasons using the SMOS data on its thermal microwave emission at a frequency of 1.4 GHz. The major feature of the proposed retrieving method is employing the temperature-dependent dielectric model of frozen arctic soil as part of the used land surface brightness model, thus linking the microwave brightness temperature observed in a certain range of viewing angles to the temperature profile in the topsoil. The experimental validation of the proposed retrieval method was conducted with the use of SMOS brightness temperature data corresponding to the DGG node closest to the TFS in the area of North Slope, Alaska, spanning a time period from January 1, 2010 to December 31, 2011. Comparison of temperature data at depths of 0.6, 8.7, and 16 cm calculated from retrieved surface temperatures, i.e., T_s , and temperature gradients, i.e., T_g , with respective *in situ* soil temperatures taken at the TFS weather station revealed rmse values of 2.8 °C, 4.9 °C, and 6.4 °C and R^2 values of 0.62, 0.42, and 0.26, respectively.

These estimates verify that the SMOS data have a potential for monitoring the topsoil temperature in a topsoil of the arctic tundra, particularly near the soil surface at a depth of 0.6 cm. At the same time, the temperatures retrieved with the SMOS data at larger depths of 8.7 and 16 cm have a rather large error when used in practice. Nevertheless, the proposed method has the potential of decreasing its error by taking into account some more factors in the used brightness temperature model. For this purpose, we plan to introduce the following factors: 1) developing dielectric models adequate for the soil types comprising the SMOS footprint area; 2) introducing the effects of open water objects; 3) taking into account the impact of snow and vegetation covers; and finally, 4) conducting experimental tests at several test sites located in tundra areas with varying physiographic characteristics.

REFERENCES

- [1] S. Hachem, C. R. Duguay, and M. Allard, "Comparison of MODIS-derived land surface temperatures with ground surface and air temperature measurements in continuous permafrost terrain," *The Cryosphere*, vol. 6, pp. 51–69, 2012, doi: 10.5194/tc-6-51-2012.
- [2] L. A. Jones, J. S. Kimball, K. C. McDonald, S. T. K. Chan, E. G. Njoku, and W. C. Oechel, "Satellite microwave remote sensing of boreal and arctic soil temperatures from AMSR-E," *IEEE Trans. Geosci. Remote Sens.*, vol. 45, no. 7, pp. 2004–2018, Jul. 2007.
- [3] S. Zhao, L. Zhang, T. Zhang, Z. Hao, L. Chai, and Z. Zhang, "An empirical model to estimate the microwave penetration depth of frozen soil," in *Proc. IEEE IGARSS*, 2012, pp. 4493–4496.
- [4] K. Rautiainen *et al.*, "L-band radiometer observations of soil processes in boreal and subarctic environments," *IEEE Trans. Geosci. Remote Sens.*, vol. 50, no. 5, pp. 1483–1497, May 2012.
- [5] V. L. Mironov, K. V. Muzalevskiy, and I. V. Savin, "Retrieving temperature gradient in frozen active layer of arctic tundra soils from radiothermal observations in L-band—Theoretical modeling," *IEEE J. Sel. Topics Appl. Earth Observ. Remote Sens.*, vol. 6, no. 3, pp. 1781–1785, Jun. 2013.
- [6] J. Wigneron *et al.*, "Evaluating an improved parameterization of the soil emission in L-MEB," *IEEE Trans. Geosci. Remote Sens.*, vol. 49, no. 4, pp. 1177–1189, Apr. 2011.
- [7] V. L. Mironov, R. D. De Roo, and I. V. Savin, "Temperature-dependable microwave dielectric model for an arctic soil," *IEEE Trans. Geosci. Remote Sens.*, vol. 48, no. 6, pp. 2544–2556, Jun. 2010.
- [8] "Toolik, Alaska database," USDA Natural Resour. Conservation Serv., Washington, DC, USA, 2014. [Online]. Available: http://www.nrcs.usda.gov/wps/portal/nrcs/detail/soils/home/?cid=NRCS142P2_053712
- [9] P. F. Sullivan, M. Sommerkorn, H. M. Rueth, K. J. Nadelhoffer, G. R. Shaver, and J. M. Welker, "Climate and species affect fine root production with long-term fertilization in acidic tussock tundra near Toolik Lake, Alaska," *Oecologia*, vol. 153, pp. 643–652, 2007.
- [10] "Biocomplexity of patterned ground. Data report. Dalton Highway," Alaska Geobotany Center, Fairbanks, AK, USA, Data Rep., 2001–2005. [Online]. Available: http://www.geobotany.org/library/reports/BarredaJE2006_daltonhwy_20060301.pdf
- [11] Y. H. Kerr *et al.*, "The SMOS mission: New tool for monitoring key elements of the global water cycle," *Proc. IEEE*, vol. 98, no. 5, pp. 666–687, May 2010.
- [12] A. Camps, M. Vall-llossera, N. Duffo, F. Torres, and I. Corbella, "Performance of sea surface salinity and soil moisture retrieval algorithms with different auxiliary datasets in 2-D L-band aperture synthesis interferometric radiometers," *IEEE Trans. Geosci. Remote Sens.*, vol. 43, no. 5, pp. 1189–1200, May 2005.
- [13] J. P. Wigneron *et al.*, "L-band Microwave Emission of the Biosphere (L-MEB) model: Description and calibration against experimental data sets over crop fields," *Remote Sens. Environ.*, vol. 107, pp. 639–655, 2007.
- [14] H. Lawrence, J.-P. Wigneron, F. Demontoux, A. Mialon, and Y. H. Kerr, "Evaluating the semiempirical H - Q model used to calculate the L-Band emissivity of a rough bare soil," *IEEE Trans. Geosci. Remote Sens.*, vol. 51, no. 7, pp. 4075–4084, Jul. 2013.
- [15] L. M. Brekhovskikh, *Waves in Layered Media*. New York, NY, USA: Academic, 1960, p. 561.
- [16] A. Mialon, L. Coret, Y. H. Kerr, F. Secherre, and J.-P. Wigneron, "Flagging the topographic impact on the SMOS signal," *IEEE Trans. Geosci. Remote Sens.*, vol. 46, no. 3, pp. 689–694, Mar. 2008.
- [17] G. H. Golub and C. F. Van Loan, *Matrix Computations*, 3rd ed. Baltimore, MD, USA: The Johns Hopkins Univ. Press, 1996.
- [18] V. Mironov and I. Savin, "A temperature-dependent multi-relaxation spectroscopic dielectric model for thawed and frozen organic soil at 0.05–15 GHz," *Phys. Chem. Earth, A/B/C*, vol. 83/84, pp. 57–64, Mar. 14, 2015.
- [19] V. L. Mironov, I. P. Molostov, and V. V. Scherbinin, "Dielectric model of a mineral arctic soil thawed and frozen at 0.05–15 GHz," in *Proc. Int. SIBCON*, May 21–23, 2015, pp. 1–7.
- [20] K. V. Muzalevskiy and L. Yury, "Effects of organo-mineral structure of arctic topsoil on the own thermal radiation in the L-band," in *Proc. Int. SIBCON*, May 21–23, 2015, pp. 1–4.
- [21] M. Schwank *et al.*, "Snow density and ground permittivity retrieved from L-band radiometry: A synthetic analysis," *IEEE J. Sel. Topics Appl. Earth Observ. Remote Sens.*, vol. 8, no. 8, pp. 3833–3845, Aug. 2015.
- [22] J. Lemmetyinen *et al.*, "Snow density and ground permittivity retrieved from L-band radiometry: Application to experimental data," *Remote Sens. Environ.*, vol. 180, pp. 377–391, Jul. 2016.
- [23] J. Lemmetyinen, J. Pulliainen, A. Rees, A. Kontu, Q. Yubao, and C. Derksen, "Multiple-layer adaptation of HUT snow emission model: Comparison with experimental data," *IEEE Trans. Geosci. Remote Sens.*, vol. 48, no. 7, pp. 2781–2794, Jul. 2010.
- [24] P. P. Bobrov, V. L. Mironov, and A. S. Yashchenko, "Diurnal dynamics of soil brightness temperatures observed at frequencies of 1.4 and 6.9 GHz in the processes of freezing and thawing," *J. Commun. Technol. Electron.*, vol. 55, no. 4, pp. 395–402, 2010.
- [25] M. Fily, A. Royer, K. Goita, and C. Prigent, "A simple retrieval method for land surface temperature and fraction of water surface determination from satellite microwave brightness temperatures in sub-arctic areas," *Remote Sens. Environ.*, vol. 85, pp. 328–338, 2003.



Valery L. Mironov (M'98) received the M.S. and Ph.D. degrees in radio science and electronics from Tomsk State University, Tomsk, Russia, in 1961 and 1968, respectively.

As a scientist, he was with the Siberian Institute of Physics and Engineering from 1961 to 1970 and the Institute of Atmospheric Optics of the Siberian Branch of the Russian Academy of Sciences (SB RAS) from 1970 to 1986. He was a Deputy Director of the Institute of Atmospheric Optics of the SB RAS from 1982 to 1986 and the President of Altai State University, Barnaul, Russia, from 1986 to 1997. He was a Visiting Scientist with The University of British Columbia, Vancouver, BC, Canada, during 1997–1998 and with the Geophysical Institute, University of Alaska, Fairbanks, AK, USA, in 2001, where he received a position of Affiliate Professor in Geophysics. In 2002, he was a Visiting Lecturer with the Radiation Laboratory, University of Michigan, Ann Arbor, MI, USA. He is currently a Senior Scientist and a Department Head with the Krasnoyarsk Scientific Center of the SB RAS, Krasnoyarsk, Russia. He is the author/coauthor of over 250 scientific publications and six books titled *Microwave Remote Sensing of Soils* (Publishing House of the Siberian Branch of the Russian Academy of Sciences, 2000; in Russian), *Lidar in a Turbulent Atmosphere* (Artech House, 1987), *Optical Remote Sensing of the Turbulent Atmosphere* (Nauka, 1986; in Russian), *Laser Coherence in a Turbulent Atmosphere* (Nauka, 1985; in Russian), *Laser Beam Propagation in a Turbulent Atmosphere* (Nauka, 1981; in Russian), and *Laser in a Turbulent Atmosphere* (Nauka, 1976; in Russian). His current research interests include electromagnetic wave propagation and scattering, microwave remote sensing, soil dielectric properties modeling, radiometry, and SAR data processing algorithms. He has also contributed to research in laser beam propagation and imaging through a turbulent atmosphere, lidar remote sensing of the atmosphere, electromagnetic surface wave scattering, and waveguide studies. In particular, he coauthored the discovery and interpretation of the radar backscattering enhancement effect in 1972.

Dr. Mironov has been a member of the Physics and Engineering Board at the SB RAS since 1985. He has been the Chairman of the Ph.D. Award Council in Physics, Mathematics and Engineering at Altai State University since 1997. He has served as a member of the Editorial Board of *Earth Observation and Remote Sensing* from 1993 to 1997 and *Higher Education in Russia* from 1995 to 1998, published in Russia. He was an Altai State Science and Engineering Prize winner in 1999. In 1987, he was granted an Award in Applied Research from the SB RAS. In 1985, he was a winner of the USSR State Prize in Science and Engineering. In 1997, he was granted a status of Honorable Professor of Altai State University. He is a member of the Russian Academy of Sciences and the Russian Academy of Higher Education.



Konstantin V. Muzalevskiy (M'12) received the M.S. degree in radio science and electronics from Altai State University, Barnaul, Russia, in 2004 and the Ph.D. degree in radiophysics from the Kirensky Institute of Physics, Siberian Branch of the Russian Academy of Sciences (SB RAS), Krasnoyarsk, Russia, in 2010.

Since 2008, he has been an Assistant Professor with the M.F. Reshetnev Siberian State Aerospace University, Krasnoyarsk. Since 2010, he has been a Research Fellow with the Laboratory of Radiophysics of Remote Sensing, Kirensky Institute of Physics, SB RAS. He is the author/coauthor of over 40 scientific publications and a book. As a young scientist, he had been supported by the Krasnoyarsk Regional Foundation for Support of Scientific and Technological Activities (2010, 2011, and 2015), The Mikhail Prokhorov Foundation (2010), the Foundation for Assistance to Small Innovative Enterprises in Science and Technology Grant (2009), and the Russian Foundation for Basic Research (2009 and 2012). He is the leader of the youth projects devoted to developing the remote sensing technologies of soil temperature and soil moisture monitoring in the Arctic tundra regions during the freezing and thawing process.



Zdenek Ruzicka received the Master's degree in geoinformatics from the Czech Technical University, Prague, Czech Republic, in 2012.

He is currently an Engineer Researcher with the Kirensky Institute of Physics, Siberian Branch of the Russian Academy of Sciences, Krasnoyarsk, Russia, and a postgraduate with the Siberian State Aerospace University, Krasnoyarsk. His research interests include geoinformatics and processing of remote sensing data.